Supplementary materials

Antibiotic stress selects against cooperation in the pathogenic bacterium *Pseudomonas aeruginosa*

Marie Vasse[a,1], Robert Noble[a,1], Andrei R. Akhmetzhanov[a,b], Clara Torres-Barceló[a], James Gurney[a], Simon Benateau[a], Claire Gougat-Barbera[a], Oliver Kaltz[a], Michael E. Hochberg[a,c]

[1] co-first authors

a. Institut des Sciences de l'Evolution, CNRS-Université de Montpellier, Place Eugène Bataillon, Montpellier Cedex 5 34095, France
b. Institute of Statistical Science, Academia Sinica, 128 Academia Rd, Section 2, Nankang 11529, Taipei, Taiwan
c. Santa Fe Institute, 1399 Hyde Park Road, Santa Fe, NM 87501, USA

Section 1: 48-hour experiment: experimental conditions and additional results

Materials and Methods

Bacterial strains

We used *Pseudomonas aeruginosa* PAO1 (ATCC 15692) as the pyoverdin-producing strain (hereafter called "producers") and the mutant PAO1Δ*pvdD* (1), derived from the same genetic background, as the non-producing strain (hereafter called "non-producers"). The knockout of the non-ribosomal peptide synthetase gene pvdD prevents pyoverdin production. We initiated 5 populations of producers and 5 of non-producers, each from a single arbitrarily chosen colony, in 6 mL of casamino acids medium (CAA; 5 g Casamino acids, 1.18 g $K_2HPO_43H_20$, 0.25 g $MgSo_47H_20$, per litre; Sigma-Aldrich) contained in 30 mL Thermo-Fisher microcosms. Populations were incubated overnight at 37°C under constant orbital shaking (200 rpm) before being used as inoculum for the experiment.

Experimental conditions

The experiment was carried out at 37°C under constant orbital shaking (350 rpm, 8mm stroke) to ensure well-mixed conditions. To minimize evaporation, we used the inner wells of 48-well plates as microcosms, each containing 800 µL of iron-limited CAA medium. To create the iron-limited conditions, we supplemented the CAA medium with 100 µg/mL of a strong iron chelator, human apotransferrin (Sigma-Aldrich), and 20 mM of sodium bicarbonate. We used millipore water to prepare all solutions to limit the amount of exogenous iron.

We employed the aminoglycoside antibiotic gentamicin (Sigma-Aldrich) at final concentrations of 2, 4 or 8 µg/mL to assess the impact of increasing antibiotic pressure. In a preliminary experiment, we estimated that 10 µg/mL is the minimum gentamicin concentration that prevents *P. aeruginosa* growth under our experimental conditions. Briefly, we initiated 12 replicate populations of producers and 12 of non-producers in 800 µL of iron-limited CAA supplemented with increasing concentrations of gentamicin in 48-well plates with an initial density of 10^7 bacteria per mL. Plates were incubated at 37°C under constant orbital shaking at 350 rpm. After 24 hours, we read optical density (OD) of each population using a spectrophotometer (ClarioSTAR microplate reader, BMG Lab Technologies) and scored growth inhibition if $OD < 0.1$ (corresponding to the minimal value in the accurate detection range of the spectrophotometer).

Experimental protocol
We inoculated bacteria as either monocultures or mixed cultures of producers and non-producers to a final density of *c* 10^7 bacteria per mL into fresh medium with either a low (2 µg/mL), intermediate (4 µg/mL), or high (8 µg/mL) dose of gentamicin, or in antibiotic-free medium. Mixed populations were initiated with 15%, or 45%, or 75% of non-producers. Each treatment was replicated 5 times for a total of 100 populations (4 antibiotic conditions × 5 types of cultures × 5 replicates) that were arbitrarily distributed in the 48-well plates. The experiment was run for 48 hours. While the up- or down-regulation of pyoverdin production could have occurred, the evolution and selection of a *de novo* cheating mutant is unlikely within this timeframe.

Population densities and relative frequencies of producers and non-producers
We mixed individual populations by pipetting and sampled 20 µL of each at the beginning of the experiment (T0) and after 10 (T10), 24 (T24), 34 (T34) and 48 (T48) hours. To estimate total densities and relative frequencies, we plated serial dilutions of each sample onto King's B medium (KB) agar plates. Plates were then incubated 24 hours at 37°C for subsequent counting of colony forming units (CFUs). Numbers of bacteria were estimated by averaging the counts from at least 3 different plates. We distinguished colonies of producers from non-producers by their different colours (yellow-green and white, respectively).

Antibiotic resistance
We estimated the frequency of resistant cells at T0 and T48 by plating serially diluted samples of each population onto antibiotic-free KB agar plates and onto KB agar with 10 µg/mL gentamicin, simultaneously. We calculated the frequency of resistant cells as the ratio of the number of colonies able to grow on gentamicin-agar to the total number of colonies, with a detection threshold of 40 resistant cells (i.e. at least 1 CFU in the undiluted 20 µL sample from the 800 µL culture). We distinguished producers from non-producers based on the colour difference as described above and we further checked the phenotype of the resistant colonies by inoculating a sample of each individual colony into iron-limited CAA overnight and measuring fluorescence: producer cultures showed significantly higher fluorescence than non-producers (two-sample t test, $p < 0.001$).
To investigate the observed effects in more detail, we repeated the experiment for a subset of treatments. Using the highest dose of gentamicin (8 µg/mL), we tested monocultures of producers and non-producers, as well as mixed cultures with initially 15% of non-producers. We estimated the densities and the relative frequencies of non-producers, and the relative frequencies of resistant cells in both producer and non-producer subpopulations, by plating at T0 and T48, as described above.

Additional results

Effects of the antibiotic and initial non-producer frequency on bacterial densities
We used standard least-square methods (ANOVA) to analyse variation in final (log-transformed) bacterial density. In addition to antibiotic treatment and initial non-producer frequency, we also fitted initial density in each replicate population as a covariate. Analyses were carried out separately for producers and non-producers, as well as for the total population.
As expected, the addition of the antibiotic slowed bacterial growth and resulted in lower final densities in all populations compared to the control, with higher doses leading to lower densities (effect of gentamicin: $F_{3,79} = 282.24$, $p < 0.0001$; Supplementary Fig. 1). There was

no statistically significant effect of initial bacterial densities on final densities ($F_{1,79} = 0.63$, $p = 0.43$).

Producers grew to lower densities in mixed cultures compared to monoculture (effect of initial frequency $F_{3,63} = 77.51$, $p < 0.0001$, contrast mixed vs mono: $p < 0.0001$, Supplementary Fig. 1B). The addition of the antibiotic enhanced this effect, in particular for the highest gentamicin dose (8 µg/mL), at which the mean final density of producers in mixed culture was about 20 times lower than in monoculture (antibiotic dose × initial frequency interaction, $F_{9,63} = 10.84$, $p < 0.0001$). Indeed, at this dose, producers in mixed culture not only had lower densities than in monoculture, but also decreased in total numbers during the course of the experiment (Supplementary Fig. 2).
Conversely, non-producers reached higher final densities in mixed cultures compared to monocultures, both in the presence and absence of the antibiotic (effect of initial frequency: $F_{3,63} = 18.28$, $p < 0.0001$, contrast mixed vs. mono: $p < 0.05$, Supplementary Fig. 1C). The significant interaction between gentamicin dose and initial non-producer frequency ($F_{9,63} = 4.21$, $p < 0.001$) indicates that this mixed culture advantage was influenced by the experimental treatments, whereby there was no consistent mixed culture advantage at the lowest gentamicin dose (2 µg/mL), nor at the lowest initial frequency of non-producers (15%). However, when we repeated the experiment for 15% mixes, but at 8 µg/mL gentamicin, non-producers did grow to higher densities than in monoculture (Supplementary Fig. 4C), similar to the 45% and 75% mixes in the main experiment.
When examining the combined final density of producers and non-producers in the mixes, we found a significant interaction between antibiotic dose and initial producer frequency ($F_{12,79} = 5.64$, $p < 0.0001$). Specifically, at the two highest doses (4 µg/mL and 8 µg/mL) the total number of producers and non-producers in the mixed cultures was significantly higher than in either monoculture (mixed vs. mono contrasts: $p < 0.003$; Supplementary Fig. 1A). At the lowest dose and without the antibiotic, there were no consistent overall differences between mixed and monocultures (Supplementary Fig. 1A).

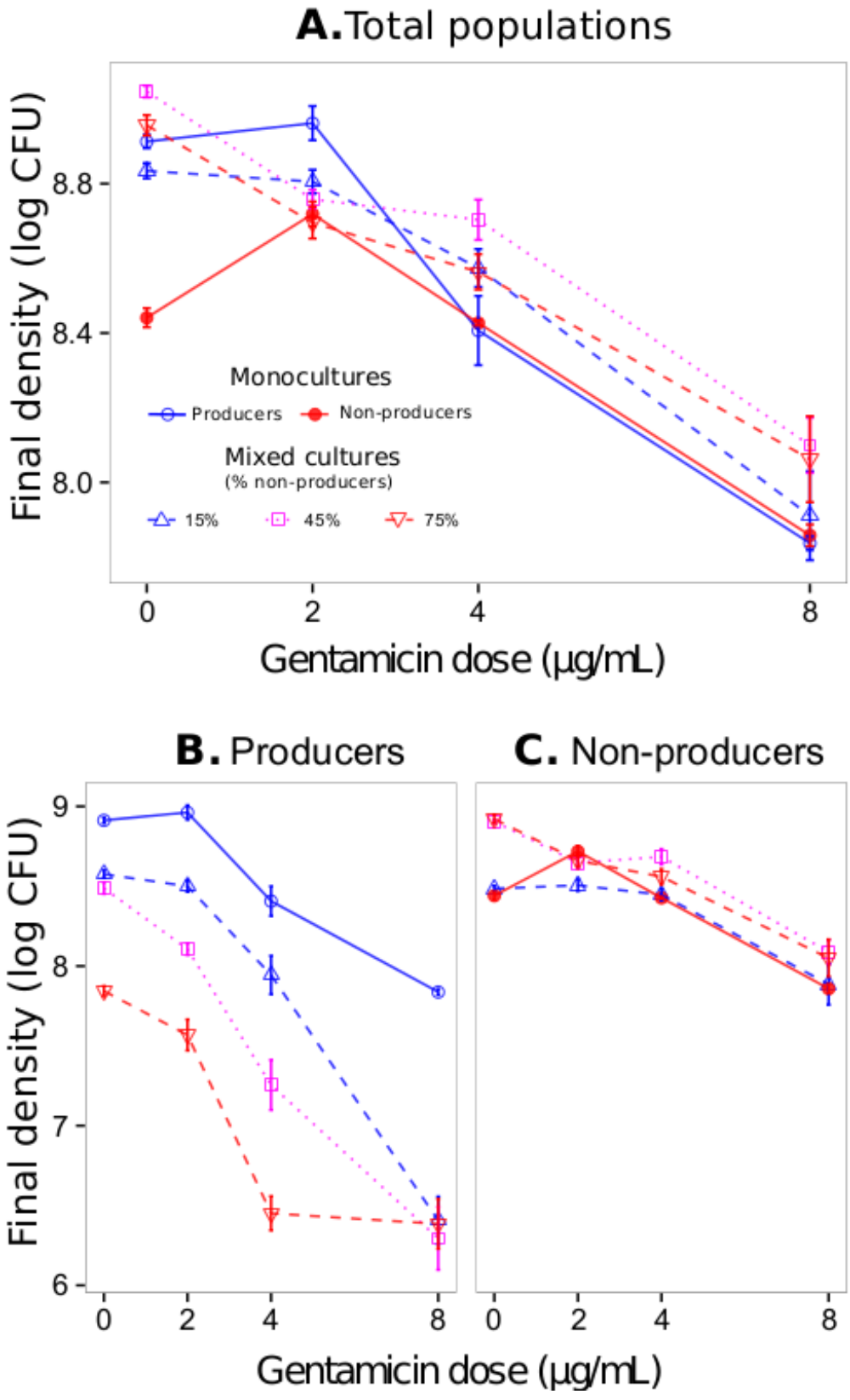

Supplementary Fig. 1: Bacterial final densities in experimental populations at T48.
Final density of total populations (**A**), producers (**B**), and non-producers (**C**) in monocultures (solid lines) and in mixed cultures (dashed lines) for different doses of gentamicin. Data are log-transformed CFUs and bars are standard errors of the mean.

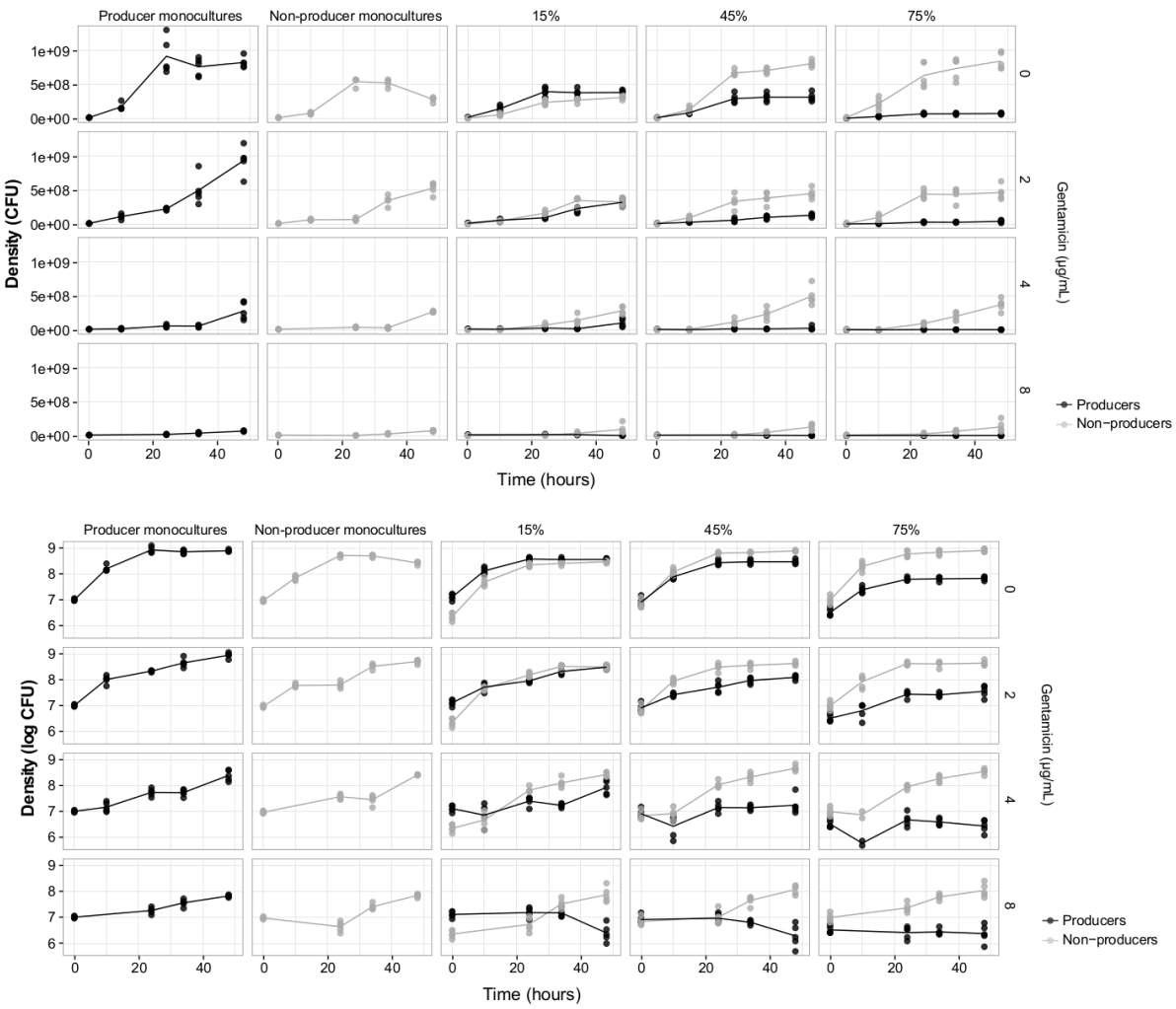

Supplementary Fig. 2: Density dynamics in experimental populations between T0 and T48. Densities (upper panel) and log-transformed densities (lower panel) of producers (black) and non-producers (grey) over the course of the experiment. Lines connect the means. Each row represents an antibiotic treatment: 0 µg/mL (first row), 2 µg/mL (second row), 4 µg/mL (third row) and 8 µg/mL of gentamicin (fourth row). The first two columns are monocultures and the last three columns are mixed cultures starting with 15%, 45% and 75% of non-producers, respectively.

Section 2: repeated 48-hour experiment and additional assays on individual colonies

a) Repeated 48-hour experiment

We initiated three replicate populations of either monocultures of producers or monocultures of non-producers or mixed cultures with 15% non-producers. The experimental conditions were the same as in the main experiment except that we used two antibiotic doses (0 µg/mL and 8 µg/mL) instead of four. We estimated the relative frequencies of each bacterial type (Supplementary Fig. 3A), their densities (Supplementary Fig. 3B-D), and the frequency of resistant cells (Supplementary Fig. 3E-G) by plating and counting CFUs at T0 and T48.
At the end of this 48-hour experiment, we arbitrarily chose up to: five individual resistant colonies from each monoculture population, 5 resistant colonies of each bacterial type from each mixed culture, and 3 non-resistant colonies of one replicate of each treatment. Additionally, 5 resistant and 5 non-resistant colonies were isolated from each replicate ancestral population. The resistant colonies were isolated from KB agar plates with 10 µg/mL of gentamicin. The non-resistant colonies were identified by introducing small samples of individual colonies, each onto both KB agar and KB agar + 10 µg/mL gentamicin plates. Those that grew on the antibiotic-free plates but not on the antibiotic plates were scored as non-resistant. Each isolated colony was inoculated in 200 µL of iron-limited CAA medium and incubated at 37°C overnight under constant orbital shaking (700 rpm) and then frozen in 20% glycerol at -80°C. These frozen stocks were then used in assays to evaluate resistance to gentamicin, population growth, and pyoverdin production.

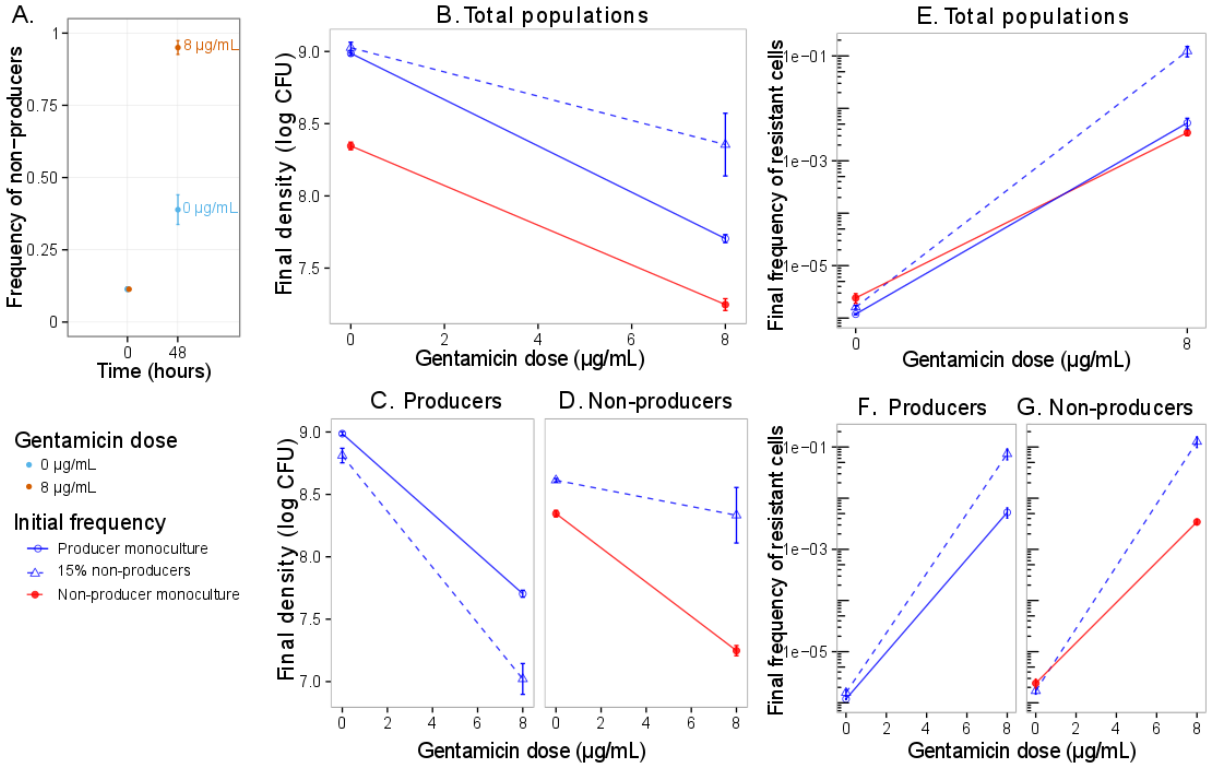

Supplementary Fig. 3: Results of the repeated 48-hour experiment.
Change in non-producer frequencies (**A**) in antibiotic-free medium (blue) and antibiotic-supplemented medium (8 µg/mL, red). Final density of total populations (**B**), producers (**C**), and non-producers (**D**) in monocultures (solid lines) and in mixed culture (dashed line) for different doses of gentamicin. Final frequency of resistant cells in total populations (**E**), in producers (**F**), and non-producers (**G**) in monocultures (solid lines) and in mixed culture (dashed line) for different doses of gentamicin. All bars are standard errors of the mean.

b) Level of resistance to gentamicin

The level of resistance to gentamicin was measured as the Minimum Inhibitory Concentration (MIC) at which no bacterial growth is detected. A sample of frozen stock from each previously isolated colony was inoculated with a sterile loop in 200 µL of iron-limited CAA medium and incubated at 37°C overnight under constant orbital shaking (700 rpm). All populations were then adjusted to an OD of 0.1 and 10 µL of each population was inoculated into 200 µL of iron-limited CAA medium with the antibiotic at two-fold increments (tested concentrations: 0, 2, 4, 8, 16 and 32 µg/mL gentamicin). After 24 hours of incubation at 37°C under constant shaking (700 rpm), we recorded the optical density (OD) of each population using a spectrophotometer (ClarioSTAR microplate reader, BMG Lab Technologies) and scored growth inhibition as OD < 0.1. We assigned a rank value of MIC to each colony as follows: MIC of 2 µg/mL = rank 1, MIC of 4 µg/mL = rank 2, MIC of 8 µg/mL = rank 3, MIC of 16 µg/mL = rank 4, MIC of 32 µg/mL = rank 5 (Supplementary Fig. 4A-C).

c) Growth and pyoverdin production

We inoculated a loop of each frozen stock into 200 µL of iron-limited CAA medium and incubated the cultures at 37°C overnight under constant orbital shaking (700 rpm). We adjusted all overnight populations to an OD of 0.1 with minimum salt solution (M9) and inoculated 10 µL of each population into an antibiotic-free iron-limited CAA medium and an iron-limited CAA supplemented with 8 µg/mL of gentamicin in clear-bottom black 96-well plates. Optical density (OD_{600}) and fluorescence (relative fluorescence unit RFU, excitation: 400 nm, emission: 460 nm) were measured every 30 minutes using the spectrophotometer for 24 hours under constant shaking (700 rpm) at 37°C.

Growth

We estimated the growth of each colony as the area under the curve (AUC) of OD_{600} over time in antibiotic-free and antibiotic-supplemented media (Supplementary Figs. 4D-F and 4G-I, respectively). The cost of antibiotic resistance is the difference in growth between resistant and non-resistant individuals in the absence of gentamicin.

Pyoverdin availability and production per producer cell

We calculated the pyoverdin availability per cell at each time point as the ratio of fluorescence to OD (RFU_t/OD_t, Supplementary Fig. 5A), and the rate of pyoverdin production as the ratio in the change in fluorescence to OD $(RFU_{t+1} - RFU_t)/OD_{t+1}$ (Supplementary Fig. 5B) (2). We excluded the data from the first 5 hours since the OD values were under the detection threshold of the spectrophotometer.

d) Genetic analysis of gentamicin resistance

We investigated the underlying genetic component of gentamicin resistance by analysing the efflux pump MexXY and 8 degrading enzymes. Bacterial DNA was obtained by boiling a sample of each colony at 95°C for 5 min in 150 µL of water. The clones used in the genetic analyses were isolated as described above and are listed in Supplementary Table 1.

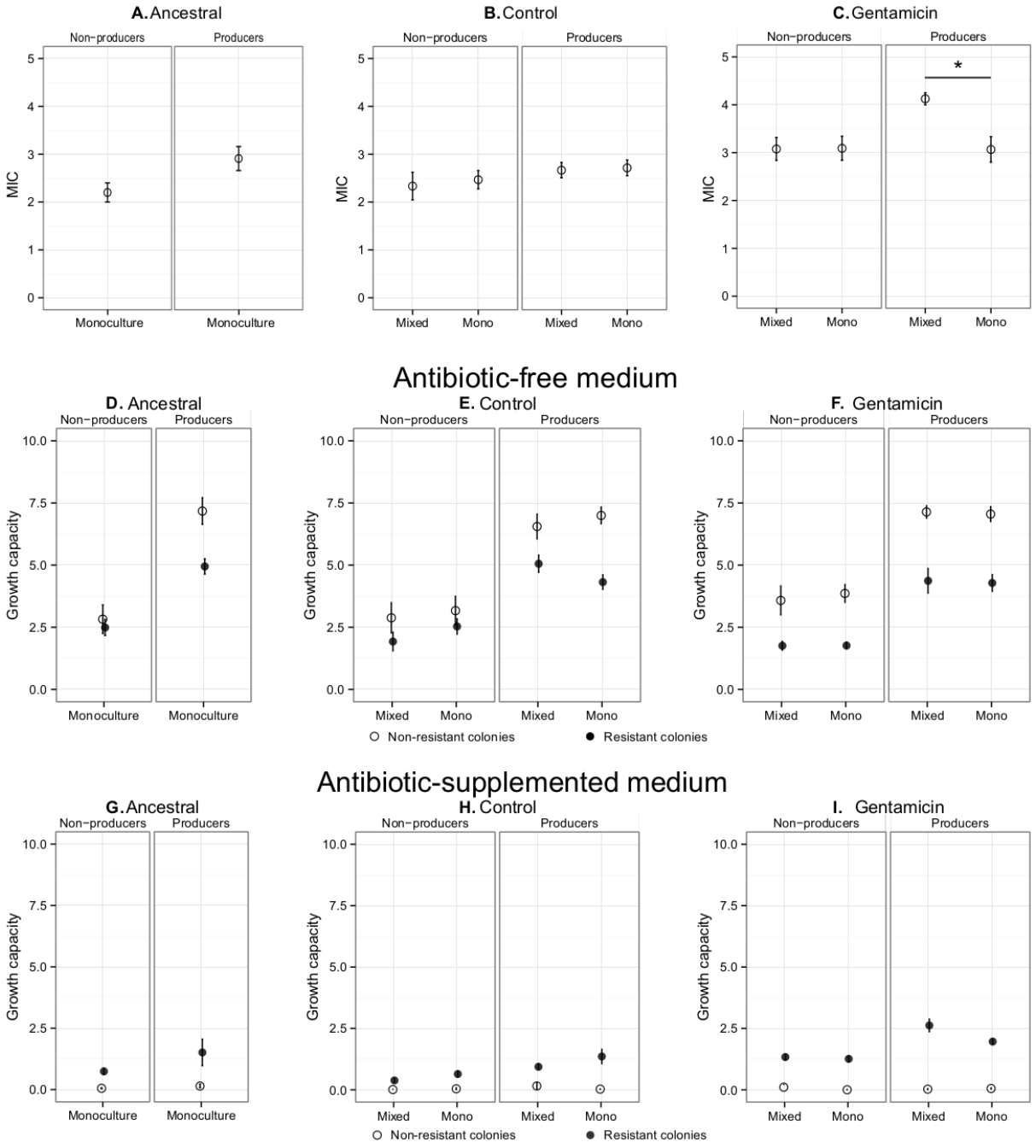

Supplementary Fig. 4: Level of resistance and growth of ancestral and evolved bacteria.
[First panel] Minimum inhibitory concentration (MIC) of individual colonies of producers and non-producers, isolated from monocultures and mixed cultures in (**A**) ancestral colonies, (**B**) colonies isolated from the evolved control populations at T48, i.e. the populations that grew without gentamicin, and (**C**) colonies isolated from the evolved treated populations at T48, i.e. those growing with 8 µg/mL gentamicin. Data are ranked values of MIC and bars are standard errors of the mean. Stars indicate a significant difference between ranked values of MIC ($p < 0.05$). [Second panel] Growth in antibiotic-free medium of individual resistant (black disks) and non-resistant (white circles) colonies of producers and non-producers, isolated from monocultures and mixed cultures in (**D**) ancestral colonies, (**E**) colonies isolated from the evolved control populations at T48, i.e. the populations that grew without gentamicin, and (**F**) colonies isolated from the evolved treated populations at T48, i.e. the populations that grew with 8 µg/mL gentamicin. [Third panel] Growth in antibiotic-supplemented medium (8 µg/mL) of individual resistant (black disks) and non-resistant (white circles) colonies of producers and non-producers, isolated from monocultures and mixed cultures in (**G**) ancestral colonies, (**H**) colonies isolated from the evolved control populations at T48, i.e. the populations that grew without gentamicin, and (**I**) colonies isolated from the evolved treated populations at T48, i.e. the populations that grew with 8µg/mL gentamicin. Data are area under the curves of OD_{600} over time and all bars are standard errors of the mean.

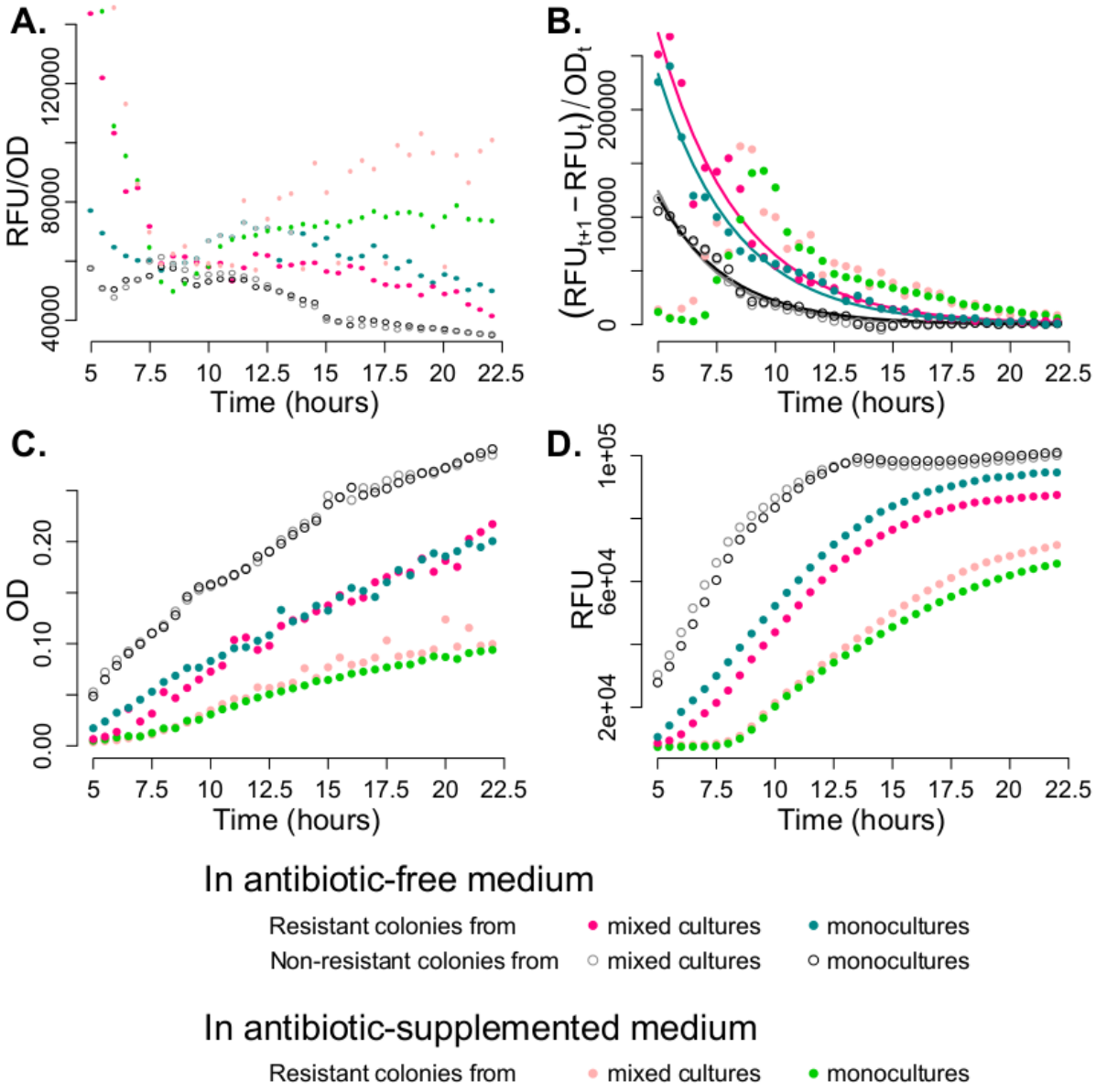

Supplementary Fig. 5: Pyoverdin availability, growth, and pyoverdin production in the presence (8 µg/mL) and in the absence of antibiotics.
Pyoverdin availability (**A**), pyoverdin production (**B**), bacterial growth (**C**), and pyoverdin concentration (**D**) were measured in 23-hour growth assays in antibiotic-free (dark pink, cyan, grey and black) and antibiotic-supplemented (pale pink and green) media. Data are averaged for 8 to 15 colonies isolated from monocultures (cyan, black and green) and mixed cultures (dark pink, grey and pale pink), resistant (dark pink and cyan; pale pink and green) and non-resistant (grey and black) to gentamicin. All colonies were isolated from the populations that evolved with 8 µg/mL gentamicin. Pyoverdin availability per producer cell was estimated as the ratio of fluorescence (relative fluorescent unit RFU) to optical density (OD_{600}). Pyoverdin production per producer cell was estimated as the ratio of the gradient of fluorescence (RFU_{t+1} - RFU_t) to optical density (OD_{600}). OD_{600} values are below the spectrophotometer detection threshold between 0 and 5 hours.

Supplementary Table 1: Clones used the genetic analyses
The clone identification corresponds to the replicate population number followed by the clone number. For example, clone 1.3 is the clone number 3 isolated from replicate population 1 (in a given treatment). For each treatment, MIC values are identical for all clones unless specified otherwise. When MIC < 2, the clones grew in the absence of gentamicin but did not grow in the presence of antibiotics, with the lowest dose tested being 2 µg/mL.

	Population	Phenotype	Clone	MIC (µg/mL)
Ancestor	na	Producer	1.3	<2
		Non-producer	1.3	<2
Evolved without gentamicin	Monoculture	Producer	2.1, 3.1	<2
		Non-producer	2.1, 3.1	<2
	Mixed culture	Producer	2.1, 3.1	<2, 4
		Non-producer	2.1, 3.1	<2
Evolved with gentamicin	Monoculture	Producer	1.1, 1.2, 2.3, 3.1	16
		Non-producer	1.1, 1.2, 2.1, 3.3	16 (clone 1.2: MIC = 4)
	Mixed culture	Producer	1.1, 1.2, 1.3, 2.1, 2.2, 2.3, 3.1, 3.2	16 (clone 2.1: MIC = 32)
		Non-producer	1.2, 2.1, 2.2, 2.3, 2.4, 2.5, 3.1, 3.2, 3.3	8, 16, 16, 16, 4, 16, 16, 4, 16

Sequencing of the MexXY efflux pump repressor
We amplified and sequenced the repressor gene *mexZ* and the intergenic region between *mexZ* and *mexX,* using the primers p819 (5'- GCA CCT GAT GGC GGA CGA -3') and p2071 (5'- GCA GCC CAG CAG GAA TAG -3') (3). Amplification by Polymerase Chain Reaction (PCR) was performed in mixtures (50 µL) containing the Taq buffer (1x), 1mM $MgCl_2$, 100 µM of each deoxynucleotide, 0,2 µM of each primer, bacterial DNA and 2 U of *Taq* polymerase (Gotaq, Promega). PCR followed a program of 1 cycle at 94°C for 5 min, 30 cycles consisting of 94°C for 30s, 65°C for 40s and 72°C for 50s, followed by a final cycle of 72°C for 10 min. The resulting 861 nucleotides product was purified and sequenced by the University of Montpellier Environmental genomics CeMEB Platform in France (Sanger sequencing). Nucleotides were aligned and compared using MEGA 6.06 software. The sequences were identical for all resistant and non-resistant clones and correspond to the *mexZ* sequence in the reference genome available on GenBank (NCBI NZ_CP017149.1).

Amplification of degrading enzymes
We tested the presence of degrading enzymes by PCR using the primers and PCR conditions reported in Supplementary Table 2. In the absence of a positive control, we cannot entirely exclude the presence of these enzymes. We used, however, primers that were shown to successfully amplify these enzymes in the same bacterial strain (4–8). No sequence was successfully amplified by any of these primers in our strains, suggesting the absence of gentamicin degrading enzymes.
Future study should elucidate the mechanisms of gentamicin resistance. This could be accomplished through whole genome sequencing of our strains to reveal a set of candidate mutations (9–15), and through determining the effect of the mutations in each genetic background.

Supplementary Table 2: Primers and PCR conditions for the amplification of degrading enzymes.

Target	Primer	Primer sequence	PCR conditions					References
			Predenaturation	Denaturation	Annealing	Elongation	Final elongation	
aac(6')-Iae	aacS1-F	5' CGCAAGCTGCAGAAATTCTAT	94°C, 5 min	94°C, 60s, 30x	50°C, 60s, 30x	72°C, 120s, 30x	72°C, 10 min	(4)
	aacS1-R	5' TCCCATTTGCATTAGGAATCA						
aac(6')-Ib	aacA4-F	5'GCTCTTGGAAGCGGGGACGG	94°C, 5 min	94°C, 60s, 30x	62°C, 60s, 30x	72°C, 120s, 30x	72°C, 10 min	(8)
	aacA4-R	5'TCGCTCGAATGCCTGGCGTG						
ant(2")-Ia	ant2bi-F	5'GACACAACGCAGGTCACATT	94°C, 5 min	94°C, 60s, 30x	60°C, 60s, 30x	72°C, 120s, 30x	72°C, 10 min	(8)
	ant2bi-R	5'CGCAAGACCTCAACCTTTC						
aph(3")-Ib	aph3bi-F	5'CTTGGTGATAACGGCAATTCC	94°C, 5 min	94°C, 60s, 30x	57°C, 60s, 30x	72°C, 120s, 30x	72°C, 10 min	(8)
	aph3bi-R	5'CCAATCGCAGATAGAAGGCAA						
ant(4')-IIb	O1	5' GAGAACCCATATGCAACATACTATCGCC	94°C, 5 min	94°C, 60s, 30x	65°C, 60s, 30x	72°C, 120s, 30x	72°C, 10 min	(7)
	O2	5' TAGAATTCTAGCGCGCACTTCGCTCTTC						
aac(6')-Ia	AAC(6')-Ia-F	5' GAATATTGCGGAATGCAG	94°C, 5 min	94°C, 60s, 30x	53°C, 60s, 30x	72°C, 120s, 30x	72°C, 10 min	(6)
	AAC(6')-Ia-R	5' GGCATTTGGAATTATTCC						
aac(6')-IIa	aac6IIa-F	5' CCATAACTCTTCGCCTCATG	94°C, 5 min	94°C, 60s, 30x	64°C, 60s, 30x	72°C, 120s, 30x	72°C, 10 min	(6)
	aac6IIa-R	5' GAGTTGTTAGGCAACACCGC						
ant(2")-Ia	ant(2")-IaF	5' ATGCGCTCACGCAACTGGTC	94°C, 5 min	94°C, 60s, 30x	65°C, 60s, 30x	72°C, 120s, 30x	72°C, 10 min	(6)
	ant(2")-IaR	5' GCATATCGCGACCTGAAAGC						
aph(3')-VI	aph(3')-VI-F	5' TCAATTCAATTCATCAAGTTT	94°C, 5 min	94°C, 30s, 30x	55°C, 30s, 30x	72°C, 60s, 30x	72°C, 5 min	(5)
	aph(3')-VI-F	5' CCGAAATGACAGTTCCTATC						

Section 3: 48-hour experiment under iron-rich conditions

To assess the impact of non-producer cheating in mixed cultures on the change in the frequency of resistant cells, we repeated the 48-hour experiment under iron-rich conditions. Under these conditions bacteria do not rely on pyoverdin production since iron is directly available.

A pilot experiment showed that adding 8 µg/mL of gentamicin in the iron-rich medium led to the extinction of all non-producer populations and approximately one-third of the producer populations. We determined that under these experimental conditions, any concentration above 6 µg/mL prevents sensitive *P. aeruginosa* growth. To limit the probability of population extinctions we therefore used gentamicin at a concentration of 5 µg/mL.

Three independent replicate colonies of both strains were inoculated in 6 mL of CAA in 30 mL Thermo-Fisher microcosms and incubated overnight under constant orbital shaking (200 rpm) at 37°C, before being used as inoculum for the 48-hour experiment. We initiated populations of either monocultures of producers or of non-producers, or mixed cultures (*c* 15% of non-producers initially) to a final density of *c* 10^7 bacteria per mL into 800 µL of CAA medium supplemented with 30 µM $Fe(III)Cl_3$ (ferric chloride, Sigma-Aldrich). Each replicate population was then inoculated in an antibiotic-free control and in an antibiotic treatment containing 5 µg/mL of gentamicin. The 48-well plates were incubated at 37°C for 48 hours under constant shaking (350 rpm). We plated serial dilutions onto KB agar and KB agar + 6 µg/mL gentamicin plates at T0 and T48 of each population to estimate the densities and the frequencies of each bacterial type (Supplementary Fig. 6A-D), and frequency of resistant cells (Supplementary Fig. 6E-G).

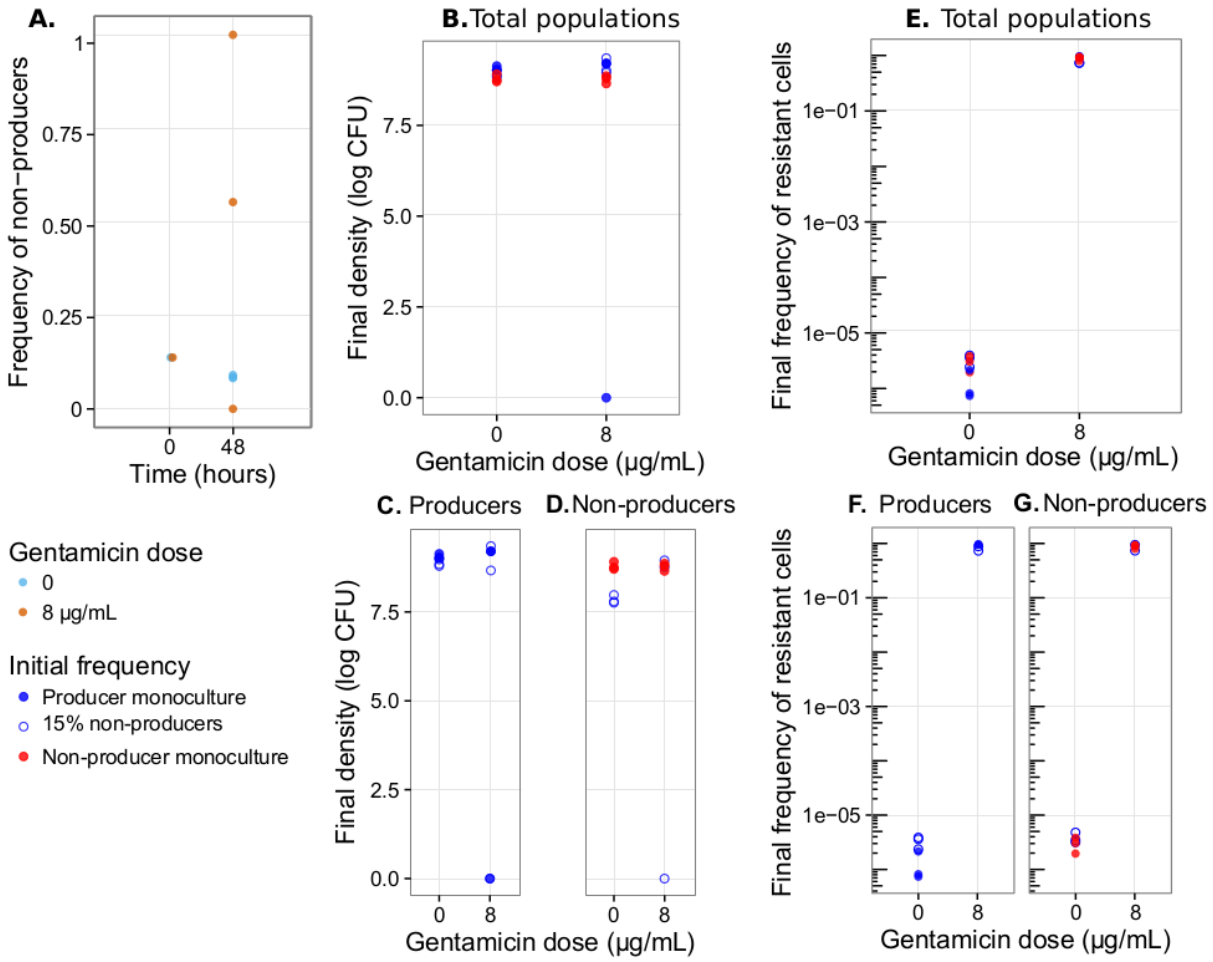

Supplementary Fig. 6: Results of the 48-hour experiment under high iron availability conditions. Change in non-producer frequencies at T0 and T48 (**A**) in antibiotic-free medium (blue) and antibiotic-supplemented medium (5 µg/mL, red). Final density of total populations (**B**), producers (**C**), and non-producers (**D**) in monocultures (red or blue disks, respectively) and in mixed culture (blue circles) for different doses of gentamicin. Data are log-transformed CFUs. Final frequency of resistant cells in in total populations (**E**), in producers (**F**) and non-producers (**G**) in monocultures (red or blue disks, respectively) and in mixed culture (blue circles) depending on gentamicin dose. In all cases, each data point represents one replicate population (3 replicates).

Section 4: Mathematical model of the effects of an ecological antagonism on public goods cooperation

To investigate the generality of our findings, we use a mathematical model of a population of public goods producers (P) and non-producers (Q), each composed of subpopulations resistant (R) and susceptible (S) to an ecological antagonism. We assume the fitness of each subpopulation X depends on the following factors: (i) the baseline birth rate, b; (ii) the cost of public goods production, α_X (for producers, α_X may depend on the public goods production rate per individual, which may in turn depend on the public goods concentration and/or total population size; for non-producers, $\alpha_X = 0$ by definition); (iii) the cost of resistance to the antagonism, β_X (for the susceptible subpopulation, $\beta_X = 0$; for the resistant subpopulation, $\beta_X = c_R$, which is constant); (iv) the population density effect, γ_X, which is relatively small when the total population size is small; (v) the benefit of public goods, δ, which increases with the public goods concentration, and is the same for all subpopulations; and (vi) the effect of the antagonism, ε_X, which depends on the level of the antagonism.
We first present a general mathematical analysis of the model. We then illustrate the consistency between the model and our experimental data by assigning specific, biologically plausible functional forms to each factor.

Analysis of how an ecological antagonism affects non-producer frequency dynamics
We are interested in how rapidly the frequency of non-producers increases during the exponential growth phase, when the population size and the public goods concentration are relatively small. We therefore assume that γ_X and δ have relatively little effect on the frequency dynamics and can be neglected, and that α_X for producers is approximately a constant, which we call c. For an antagonism that induces mortality, the dynamical equations for susceptible producers and non-producers are then, respectively,

$$\frac{dN_{PS}}{dt} = (b(1-c) - \varepsilon_{PS})N_{PS}, \qquad \frac{dN_{QS}}{dt} = \left(b - \varepsilon_{QS}\right)N_{QS}.$$

The log relative fitness of non-producers is

$$f_{QS,PS} = \varepsilon_{PS} - \varepsilon_{QS} + bc.$$

We assume a sigmoidal Hill function describes the dose-response curve of the antagonism, as has been found in studies of antibiotics including gentamicin (16–18). The general Hill function is

$$\varepsilon_X = \frac{k_X A^h}{A^h + M_X^h},$$

where A is the level of the antagonism, and k_X, h and M_X are constant parameters. Now we have

$$f_{QS,PS} = \frac{k_{PS} A^h}{A^h + M_{PS}^h} - \frac{k_{QS} A^h}{A^h + M_{QS}^h} + bc.$$

Since this expression is the difference of two sigmoidal functions, it can have at most one turning point (a point at which the derivative with respect to A changes its sign). Therefore there are four possible types of relationship between the relative fitness of non-producers and the antagonism level: monotonically increasing, monotonically decreasing, peaked (i.e. maximal at an intermediate antagonism level), or valley shaped (i.e. minimal at an intermediate antagonism level). We can distinguish between these possibilities by examining the gradient of the curve as the antagonism level, A, approaches zero and infinity. If both gradients are positive then the curve is monotonically increasing; if both are negative then it is monotonically decreasing; a switch from positive to negative means the curve is peaked; and a switch from negative to positive implies a valley shape.

Differentiating with respect to A, we find

$$\frac{\partial f_{QS,PS}}{\partial A} = \frac{k_{PS} h M_{PS}^h A^{h-1}}{(A^h + M_{PS}^h)^2} - \frac{k_{QS} h M_{QS}^h A^{h-1}}{(A^h + M_{QS}^h)^2}.$$

As A approaches zero,

$$\frac{\partial f_{QS,PS}}{\partial A} \to \frac{k_{PS} h A^{h-1}}{M_{PS}^h} - \frac{k_{QS} h A^{h-1}}{M_{QS}^h}$$
$$> 0 \text{ if and only if } \frac{k_{PS}}{k_{QS}} > \frac{M_{PS}^h}{M_{QS}^h}.$$

As A approaches infinity,

$$\frac{\partial f_{QS,PS}}{\partial A} \to \frac{k_{PS} h M_{PS}^h}{A^{h+1}} - \frac{k_{QS} h M_{QS}^h}{A^{h+1}}$$
$$> 0 \text{ if and only if } \frac{k_{PS}}{k_{QS}} > \frac{M_{QS}^h}{M_{PS}^h}.$$

The conditions for the different types of relationship are therefore as illustrated in Fig. 2. In particular, this analysis shows that non-producer frequency will increase most rapidly at an intermediate antagonism level, as in our experimental results, provided the antagonism affects producers more than non-producers at low and intermediate levels (i.e. $M_{QS} > M_{PS}$) but affects both populations similarly at very high levels (i.e. $k_{PS} \approx k_{QS}$). For values of h between 1 and 5, which apply, for example, to antibiotic dose-response curves (16, 17), the latter condition is not very restrictive; for example, if $h = 3$ and $M_{QS} / M_{PS} = 1.5$ then we require $0.29 < k_{PS} / k_{QS} < 3.4$.). In all cases, the relative fitness of non-producers is bc in the absence of the antagonism, and the relative fitness approaches the limit $bc + k_{PS} - k_{QS}$ as the antagonism level approaches infinity.

For an antagonism that slows growth or reproduction, the equations are

$$\frac{dN_{PS}}{dt} = b(1-c)(1-\varepsilon_{PS})N_{PS}, \qquad \frac{dN_{QS}}{dt} = b\left(1-\varepsilon_{QS}\right)N_{QS},$$

with $\varepsilon_{PS} \leq 1$ and $\varepsilon_{QS} \leq 1$. The criteria that determine the effects of an antagonism that slows growth or reproduction are similar to those for an antagonism that induces mortality, except that the former depend on the cost of public goods production (Fig. 2). As a numerical example, if $h = 3$, $M_{QS} / M_{PS} = 1.5$, and $c = 0.3$ then non-producer frequency will increase most rapidly at an intermediate antagonism level provided $0.42 < k_{PS} / k_{QS} < 4.8$. In all cases, the relative fitness of non-producers is bc in the absence of the antagonism, and the relative fitness approaches the limit $b(c + (1 - c)k_{PS} - k_{QS})$ as the antagonism level approaches infinity.

Analysis of public goods effect on frequency dynamics of a subpopulation resistant to an ecological antagonism

We next analyse the effect of public goods dynamics on the evolution of resistance to an ecological antagonism. We confine our analysis to the case when the level of the antagonism is high, and so the population size remains low and we can assume $\gamma_X = 0$.

Public goods concentration will affect the evolution of resistance to the antagonism only if the fitness of the resistant subpopulation, relative to the susceptible subpopulation, varies with public goods concentration. This means that the beneficial effect of public goods must interact with the effect of the antagonism or with the cost of resistance (or both). For example, consider the following model of non-producer dynamics, in which the beneficial effect of public goods and the cost of resistance have an additive effect on fitness, and the drug induces mortality:

$$\frac{dN_{QS}}{dt} = \big(b(1+\delta) - \varepsilon_{QS}\big)N_{QS}, \quad \frac{dN_{QR}}{dt} = \big(b(1-c_R+\delta) - \varepsilon_{QR}\big)N_{QR},$$

where N_{QS} is the number of susceptible non-producers, N_{QR} is the number of resistant non-producers, b is the baseline birth rate, δ is the beneficial effect of public goods, ε_X is the effect of the antagonism, and c_R is the cost of resistance. For the above model, we find that the log fitness of resistant non-producers, relative to susceptible non-producers, is

$$f_{QR,QS} = \varepsilon_{QS} - \varepsilon_{QR} - bc_R,$$

which is independent of public goods concentration. Therefore, because in this model the beneficial effect of public goods interacts with neither the cost of resistance nor the effect of the antagonism, public goods have no effect on the evolution of resistance among non-producers.

Alternatively, it is possible that the cost of resistance slows growth or reproduction, whereas the beneficial effect of public goods increases the carrying capacity. In this case, the beneficial effect of public goods and the cost of resistance have a multiplicative effect on fitness, such as

$$\frac{dN_{QS}}{dt} = \big(b\big(1-\gamma_{QS}+\delta\big) - \varepsilon_{QS}\big)N_{QS}, \quad \frac{dN_{QR}}{dt} = \big(b(1-c_R)\big(1-\gamma_{QR}+\delta\big) - \varepsilon_{QR}\big)N_{QR}.$$

When the population density effects γ_{QS} and γ_{QS} are negligible, the partial derivative of $f_{QR,QS}$ with respect to G is

$$\frac{\partial f_{QR,QS}}{\partial G} = -bc_R\frac{\partial \delta}{\partial G},$$

which is negative, because δ (the beneficial effect of public goods) is an increasing function of G (the public goods concentration). Therefore, in this case, the relative fitness of resistant non-producers decreases as public goods concentration increases. This is because the beneficial effect of public goods amplifies the difference between resistant and susceptible birth rates, in a manner analogous to negative epistasis.

If instead the effects are additive but the antagonism slows growth or reproduction then

$$\frac{\partial f_{QR,QS}}{\partial G} = b\frac{\partial \delta}{\partial G}\big(\varepsilon_{QS} - \varepsilon_{QR}\big).$$

Assuming the effect of the antagonism on the susceptible subpopulation is always larger than the effect on the resistant subpopulation (i.e. $\varepsilon_{QS} > \varepsilon_{QR}$), the above expression is positive, and so selection for resistance increases with public goods concentration.

Finally, we consider the case in which the beneficial effect of public goods and the cost of resistance have a multiplicative effect on fitness, and the antagonism slows growth or reproduction. We then find

$$\frac{\partial f_{QR,QS}}{\partial G} = b\frac{\partial \delta}{\partial G}\big((1-c_R)(1-\varepsilon_{QR}) - (1-\varepsilon_{QS})\big).$$

If the resistant subpopulation is not at all affected by the antagonism then $\varepsilon_{QR} = 0$ and the above expression will be positive provided the level of the antagonism is high enough that $\varepsilon_{QS} > c_R$. Otherwise, whether the expression is positive or negative depends on the functional forms of the effects of the antagonism. If we assume Hill functions then

$$\frac{\partial f_{QR,QS}}{\partial G} = b\frac{\partial \delta}{\partial G}\left((1-c_R)\left(1-\frac{k_{QR}A^3}{A^3+M_{QR}^3}\right) - \left(1-\frac{k_{QS}A^3}{A^3+M_{QS}^3}\right)\right).$$

It follows that if

$$(1-c_R)\left(1-\frac{k_{QR}A^3}{A^3+M_{QR}^3}\right) - \left(1-\frac{k_{QS}A^3}{A^3+M_{QS}^3}\right) > 0$$

then the relative fitness of resistant producers will increase monotonically as public goods concentration increases; otherwise it will decrease monotonically as public goods

concentration increases. The expression is the difference of two Z-shaped functions that may cross at most once. Therefore there are two possibilities: either the expression is negative for all values of A, or it is negative for small values of A, and is positive for larger values. To distinguish between these cases, we note that in the first scenario, the curve increases as A approaches infinity, whereas in the latter case the curve decreases as A approaches infinity. Differentiating with respect to A, we find

$$\frac{\partial f_{QR,QS}}{\partial G \partial A} = b\frac{\partial \delta}{\partial G}\left(\frac{k_{QS} h A^{h-1} M_{QS}^h}{(A^h + M_{QS}^h)^2} - (1-c_R)\frac{k_{QR} h A^{h-1} M_{QR}^h}{(A^h + M_{QR}^h)^2}\right)$$
$$\to b\frac{\partial \delta}{\partial G}\frac{h}{A^{h+1}}\left(k_{QS} M_{QS}^h - (1-c_R) k_{QR} M_{QR}^h\right) \text{ as } A \to \infty$$
$$< 0 \text{ if and only if } \frac{k_{QS}}{k_{QR}} < (1-c_R)\frac{M_{QR}^h}{M_{QS}^h}.$$

This tells that, at high levels of the antagonism, selection for resistance in non-producers will decrease as public goods concentration increases; otherwise, selection for resistance in non-producers will increase as public goods concentration increases. For example, if $h = 3$, $M_{QR} / M_{QS} = 5$, and $c_R = 0.3$ then we require $k_{QS} / k_{QR} < 87$.

The results for producers are qualitatively the same as for non-producers, provided the cost of public goods production is constant or decreases with increasing public goods concentration. The latter assumption is the most biologically plausible scenario, as we would expect the cost of public goods production to be a non-decreasing function of the public goods production rate per individual, and we would expect the public goods production rate per individual to be a non-increasing function of public goods concentration (due to negative feedback regulation, for example).

In summary, at high levels of an ecological antagonism, selection for resistance is predicted to increase with public goods concentration if and only if the antagonism slows growth or reproduction. This is because the beneficial effects of the public goods accentuate the fitness difference that results from unequal effects of the antagonism on the susceptible and resistant subpopulations.

Fitting the model to data

To fit the model to data from our experiments, in which the public good is pyoverdin and the antagonism is the antibiotic gentamicin, we select particular functional forms for each of the contributory factors, based on the following assumptions:

a) The cost of pyoverdin production is proportional to the production rate. In the absence of specific data to the contrary, we make the parsimonious assumption that the efficiency of the metabolic machinery responsible for pyoverdin production is directly proportional to the number of molecules produced.
b) Population growth is logistic. Other density-dependent models are possible, but the logistic growth model is a parsimonious framework and has empirical support from past study (19).
c) The primary effect of the antibiotic is bacteriostatic, and is a sigmoidal function of antibiotic concentration. Gentamicin is classified as a bacteriocide, but its killing effect is concentration-dependent and at low doses it may be bacteriostatic (17). As an approximation, we consider that the sub-MIC doses of antibiotics used in this study modify the fission rate, and we assume no effects on the death rate. Consistent with previous studies (16–18), we use a sigmoidal Hill function to describe the relationship between the concentration of the antibiotic and its effect (20). Hill functions are used in pharmacology and biochemistry to describe effects that depend on binding between a ligand (such as an antibiotic) and a target macromolecule. The extent to which

binding is enhanced by the amount of ligand already bound is quantified by a Hill function parameter called the Hill coefficient. We assume the antibiotic effect on resistant bacteria is small enough to be neglected from the model.

d) The effect of the antibiotic decreases over time. A decrease in antibiotic effect may result from bacterial adaptation, and/or from drug degradation through the accumulation of protective compounds (such as degrading enzymes) (21, 22). We formalise this assumption as an exponential decrease in the effective antibiotic concentration.
e) The pyoverdin production rate is inversely related to pyoverdin concentration. A sigmoidal pyoverdin curve, as we observed in our experiments, may result either from pyoverdin consumption or degradation, or from a decrease in the production rate over time. Given that pyoverdin is reusable and durable over 48 hours (23), the latter hypothesis appears more plausible.
f) Pyoverdin increases both bacterial fission rate and carrying capacity (23).

The specific model therefore describes bacterial dynamics as

$$\frac{dN_{PS}}{dt} = b\left(1 - c\left(1 - \frac{G}{G_{max}}\right)\right)\left(1 - \frac{N}{K} + \frac{rG}{G+H}\right)\frac{M_{PS}^h}{A^h + M_{PS}^h}N_{PS},$$

$$\frac{dN_{QS}}{dt} = b\left(1 - \frac{N}{K} + \frac{rG}{G+H}\right)\frac{M_{QS}^h}{A^h + M_{QS}^h}N_{QS},$$

$$\frac{dN_{PR}}{dt} = b\left(1 - c_R - c\left(1 - \frac{G}{G_{max}}\right)\right)\left(1 - \frac{N}{K} + \frac{rG}{G+H}\right)N_{PR},$$

$$\frac{dN_{QR}}{dt} = b(1 - c_R)\left(1 - \frac{N}{K} + \frac{rG}{G+H}\right)N_{QR},$$

Antibiotic dynamics are described as

$$\frac{dA}{dt} = -\mu A,$$

and pyoverdin dynamics as

$$\frac{dG}{dt} = v(N_{PS} + N_{PR})\left(1 - \frac{G}{G_{max}}\right).$$

Although we did not collect data on pyoverdin concentration during the course of the competition experiments, we had pyoverdin accumulation data from the additional growth assays performed on the single antibiotic resistant and susceptible colonies isolated from evolved populations (for method details see Supplementary Information). The experimental conditions were different from the competition experiment with respect to the culture volume (200 µL for the assays and 800 µL for the competition experiment), the duration (24 hours for the assays and 48 hours for the competition experiment), and the type of populations (single colony for the assays and competition for the experiment). The rate of exponential growth was higher in the assays compared to the competition experiments and we do not know whether the pyoverdin-related parameters also differed. Accordingly, we did not combine data from the two sets of experiments. To fit the model we required only initial pyoverdin concentrations, which we set equal to the initial producer frequency (pyoverdin concentration is thus measured relative to the largest of its initial values). Alternatively setting all initial pyoverdin concentrations equal to one (in cultures containing producers) or zero (in non-producer monocultures) resulted in qualitatively similar dynamics but with a larger deviance between the model and the data.

We fitted the model to the bacterial population data using a Markov chain Monte Carlo (MCMC) method, implemented by WinBUGS with the WBDiff package for differential equation models (24, 25). An advantage of this Bayesian method is that it returns posterior

distributions instead of "best fit" parameter values, thus enabling us to assess the uncertainty of each estimate. The uncertainty can be summarised using credible intervals, which are the Bayesian equivalent of confidence intervals (26). We also verified the fit using the alternative package FME, written in R (27). Median estimates and 95% credible intervals are listed in Supplementary Table 3.

As predicted by the mathematical analysis, the model is consistent with the experimental data for the effect of antibiotic concentration on non-producer frequency dynamics (Supplementary Fig. 7). Also as predicted, the model is consistent with the experimental data for the effect of initial non-producer frequency on the evolution of resistance in non-producers, though not in producers (Fig. 1C). The sigmoidal pyoverdin curves resulting from the model are qualitatively consistent with what we observed in the growth assays.

Model comparison confirms that pyoverdin dynamics have an important influence on the population dynamics. We compared models using the deviance information criterion (DIC), a measure that takes into account both the model fit and the number of effective parameters, and which is appropriate for our MCMC method. If the DIC values of two alternative models differ by more than 10 then the model with the lower DIC is considered to have much stronger support (28). Our model with pyoverdin dynamics has a DIC value approximately 67 less than that of a model without pyoverdin dynamics.

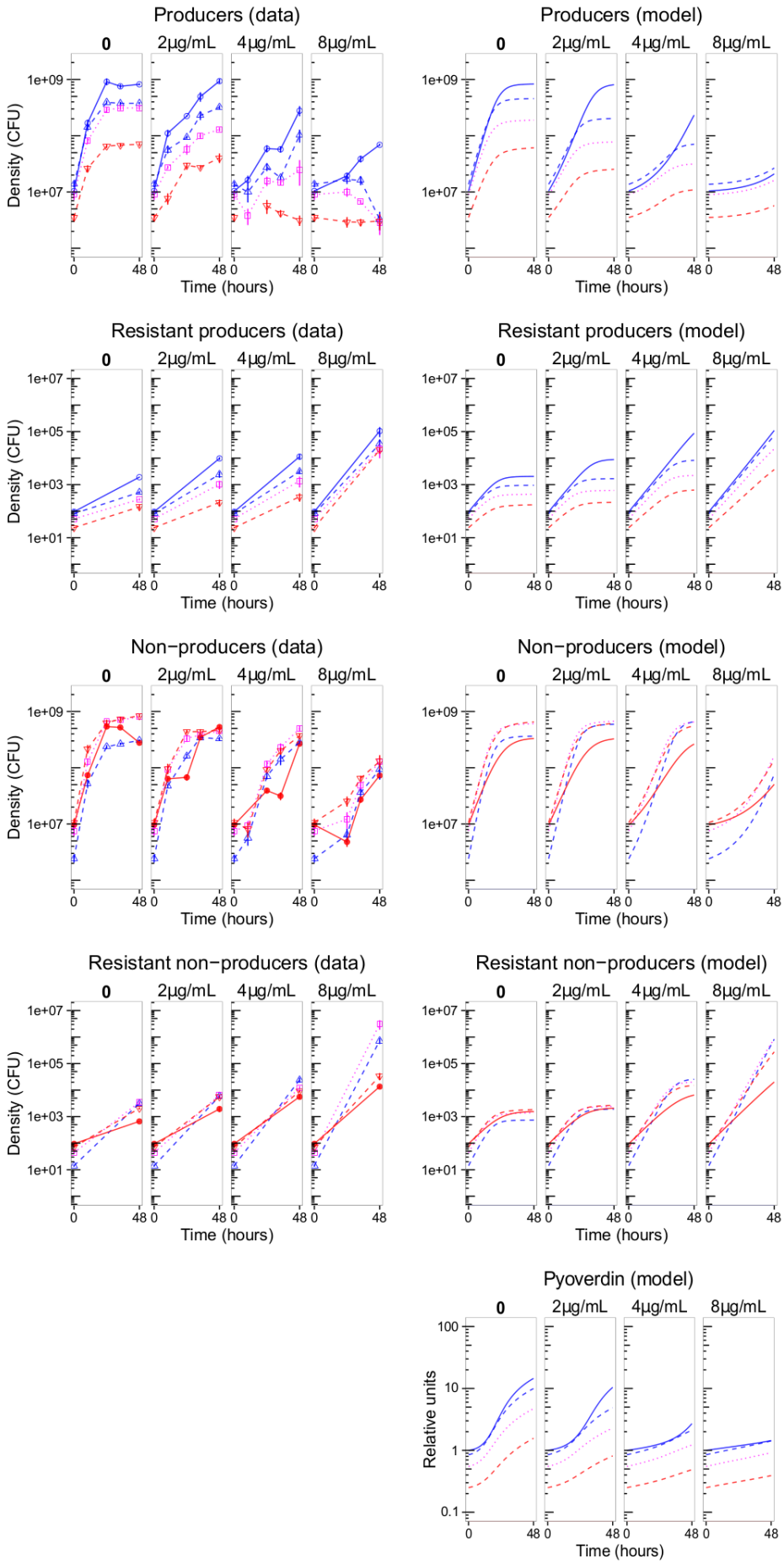
Producers (data)
Producers (model)
Resistant producers (data)
Resistant producers (model)
Non−producers (data)
Non−producers (model)
Resistant non−producers (data)
Resistant non−producers (model)
Pyoverdin (model)
0
2µg/mL
4µg/mL
8µg/mL
Density (CFU)
Relative units
Time (hours)

Supplementary Fig. 7: Experimental data (left column) and results of the mathematical model fitted to data (right column). Colours indicate initial non-producer frequencies (solid blue = 0%, dashed blue = 15%, dotted magenta = 45%, dashed red = 75%, solid red = 100%). Each set of four panels corresponds to four different gentamicin doses (0, 2, 4 and 8 μg/mL). Bars are standard errors of the mean. Parameter values as in Supplementary Table 3.

Supplementary Table 3: Model variables, parameters, and parameter values estimated from fitting to data.

Variable	Definition	
N_{PS}	Density of susceptible producers	
N_{QS}	Density of susceptible non-producers	
N_{PR}	Density of resistant producers	
N_{QR}	Density of resistant non-producers	
N	Density of the total population ($N = N_{CS} + N_{DS} + N_{CR} + N_{DR}$)	
A	Effective antibiotic concentration	
G	Pyoverdin concentration	
Parameter	Definition	Median estimate [95% credible interval]
b	Baseline fission rate	0.15 [0.12, 0.18] per hour
K	Baseline carrying capacity	3.4×10^{8} [2.7×10^{8}, 4.4×10^{8}] bacteria
c	Cost of pyoverdin production	0.31 [0.26, 0.37]
c_R	Cost of resistance	0.21 [0.12, 0.31]
M_{PS}	Antibiotic concentration at which effect is at half its maximum value	1.9 [1.5, 2.3] μg/mL
M_{QS}	Antibiotic concentration at which effect is at half its maximum value	3.3 [2.6, 4.1] μg/mL
h	Hill coefficient	2.9 [2.1, 4.4]
μ	Rate of decrease of effective antibiotic concentration	0.019 [0.0074, 0.030] per hour
v	Maximum pyoverdin production rate per cell	7.1×10^{-10} [1.6×10^{-10}, 3.2×10^{-9}] relative units per cell per hour
r	Maximum pyoverdin-dependent increase in fission rate	1.5 [1.0, 2.2]
H	Pyoverdin concentration at which effect is at half its maximum value	0.51 [0.19, 1,3] relative units
G_{max}	Pyoverdin concentration at which production ceases	49 [10, 270] relative units

References

1. Ghysels B, et al. (2004) FpvB, an alternative type I ferripyoverdine receptor of Pseudomonas aeruginosa. *Microbiology* 150(6):1671–1680.

2. Ghoul, M. (2014) Social Dynamics in Natural Populations of Pseudomonas aeruginosa. Available at: http://www.zoo.ox.ac.uk/group/west/pdf/MGhoul-THESIS-revised*.pdf.

3. Vogne C, Aires JR, Bailly C, Hocquet D, Plésiat P (2004) Role of the Multidrug Efflux System MexXY in the Emergence of Moderate Resistance to Aminoglycosides among Pseudomonas aeruginosa Isolates from Patients with Cystic Fibrosis. *Antimicrob Agents Chemother* 48(5):1676–1680.

4. Sekiguchi J, et al. (2005) Multidrug-Resistant Pseudomonas aeruginosa Strain That Caused an Outbreak in a Neurosurgery Ward and Its aac(6′)-Iae Gene Cassette Encoding a Novel Aminoglycoside Acetyltransferase. *Antimicrob Agents Chemother* 49(9):3734–3742.

5. Hu X, et al. (2013) A high throughput multiplex PCR assay for simultaneous detection of seven aminoglycoside-resistance genes in Enterobacteriaceae. *BMC Microbiol* 13:58.

6. Dubois V, et al. (2008) Beta-lactam and aminoglycoside resistance rates and mechanisms among Pseudomonas aeruginosa in French general practice (community and private healthcare centres). *J Antimicrob Chemother* 62(2):316–323.

7. Sabtcheva S, Galimand M, Gerbaud G, Courvalin P, Lambert T (2003) Aminoglycoside Resistance Gene ant(4′)-IIb of Pseudomonas aeruginosa BM4492, a Clinical Isolate from Bulgaria. *Antimicrob Agents Chemother* 47(5):1584–1588.

8. Michalska AD, Sacha PT, Ojdana D, Wieczorek A, Tryniszewska E (2014) Prevalence of resistance to aminoglycosides and fluoroquinolones among Pseudomonas aeruginosa strains in a University Hospital in Northeastern Poland. *Braz J Microbiol Publ Braz Soc Microbiol* 45(4):1455–1458.

9. Martinez JL, Baquero F (2000) Mutation Frequencies and Antibiotic Resistance. *Antimicrob Agents Chemother* 44(7):1771–1777.

10. Toprak E, et al. (2012) Evolutionary paths to antibiotic resistance under dynamically sustained drug selection. *Nat Genet* 44(1):101–105.

11. Schenk MF, de Visser JAG (2013) Predicting the evolution of antibiotic resistance. *BMC Biol* 11:14.

12. Livermore DM (2002) Multiple Mechanisms of Antimicrobial Resistance in Pseudomonas aeruginosa: Our Worst Nightmare? *Clin Infect Dis* 34(5):634–640.

13. Long H, et al. (2016) Antibiotic treatment enhances the genome-wide mutation rate of target cells. *Proc Natl Acad Sci U S A* 113(18):E2498–2505.

14. Chewapreecha C, et al. (2014) Comprehensive identification of single nucleotide polymorphisms associated with beta-lactam resistance within pneumococcal mosaic genes. *PLoS Genet* 10(8):e1004547.

15. Safi H, et al. (2013) Evolution of high-level ethambutol-resistant tuberculosis through interacting mutations in decaprenylphosphoryl-β-D-arabinose biosynthetic and utilization pathway genes. *Nat Genet* 45(10):1190–1197.

16. Regoes RR, et al. (2004) Pharmacodynamic Functions: a Multiparameter Approach to the Design of Antibiotic Treatment Regimens. *Antimicrob Agents Chemother* 48(10):3670–3676.

17. Tam VH, Kabbara S, Vo G, Schilling AN, Coyle EA (2006) Comparative Pharmacodynamics of Gentamicin against Staphylococcus aureus and Pseudomonas aeruginosa. *Antimicrob Agents Chemother* 50(8):2626–2631.

18. Udekwu KI, Parrish N, Ankomah P, Baquero F, Levin BR (2009) Functional relationship between bacterial cell density and the efficacy of antibiotics. *J Antimicrob Chemother* 63(4):745–757.

19. Kümmerli R, Jiricny N, Clarke LS, West SA, Griffin AS (2009) Phenotypic plasticity of a cooperative behaviour in bacteria. *J Evol Biol* 22(3):589–598.

20. Czock D, Keller F (2007) Mechanism-based pharmacokinetic-pharmacodynamic modeling of antimicrobial drug effects. *J Pharmacokinet Pharmacodyn* 34(6):727–751.

21. Garneau-Tsodikova S, Labby KJ (2016) Mechanisms of resistance to aminoglycoside antibiotics: overview and perspectives. *Med Chem Commun* (7):11–27.

22. Poole K (2005) Aminoglycoside Resistance in Pseudomonas aeruginosa. *Antimicrob Agents Chemother* 49(2):479–487.

23. Kümmerli R, Brown SP (2010) Molecular and regulatory properties of a public good shape the evolution of cooperation. *Proc Natl Acad Sci* 107(44):18921–18926.

24. Lunn, D.J. (2004) *WinBUGS differential interface—worked examples* (Department of Epidemiology and Public Health, Imperial College School of Medicine, London).

25. Lunn, D.J., Thomas, A., Best, N., Spiegelhalter, D. (2000) WinBUGS -- a Bayesian modelling framework: concepts, structure, and extensibility. *Stat Comput* 10:325–337.

26. J Kruschke *Doing Bayesian Data Analysis, 2nd Edition. A Tutorial with R, JAGS, and Stan* (Academic Press).

27. Soetaert K, Petzoldt T (2010) Inverse Modelling, Sensitivity and Monte Carlo Analysis in R Using Package FME. *J Stat Softw* 33(3). doi:10.18637/jss.v033.i03.

28. Spiegelhalter DJ, Best NG, Carlin BP, Van Der Linde A (2002) Bayesian measures of model complexity and fit. *J R Stat Soc Ser B Stat Methodol* 64(4):583–639.